ELSEVIER

Chemical Physics 209 (1996) 265–274

Chemical Physics

Deuteration of positive hydrogen cluster ions H_5^+ to H_{17}^+ at 10 K

W. Paul, S. Schlemmer, B. Lücke, D. Gerlich [1]

Department of Physics, Technical University Chemnitz-Zwickau, D-09107 Chemnitz, Germany

Received 3 February 1996

Abstract

The dynamics of the sequential deuteration of hydrogen cluster cations H_n^+, n odd, is studied in a 22-pole radio frequency ion trap at a nominal temperature of 10 K. Rate coefficients for the step by step replacement of hydrogen by deuterium in initially mass selected clusters, H_n^+, for $n = 3, \ldots, 17$ are extracted from the measured temporal evolution of the product ion intensities. The rates for the exchange of a single proton or alternatively for the replacement of a hydrogen molecule are strongly cluster size dependent. This is additional evidence for a previously proposed dynamical shell structure [W. Paul et al., Intern. J. Mass Spectrom. Ion Processes 150 (1995) 373]. Measurements are carried out in normal deuterium and deuterium with admixtures of helium, para hydrogen or normal hydrogen in order to investigate thermalization and the influence of back reactions. Results are discussed on the basis of calculated equilibrium structures, zero point energies and simple dynamical considerations. Constraints for intracluster rearrangement processes are found.

1. Introduction

Positive hydrogen cluster ions have been extensively studied since the seventies stimulated by the interesting properties of these simple molecular assembles [1–12]. A wide range of binding energies from several kcal/mol for the H_5^+ system to the heat of evaporation of liquid hydrogen ($\approx$ 0.2 kcal/mol) as well as size and shell effects stimulated experimental studies as well as state of the art theoretical work. A variety of ab initio calculations has been carried out at Hartree–Fock (SCF) and configuration interaction (CI, CISD) level of theory [10,11,13–16] in order to predict equilibrium geometries, vibrational frequencies, infrared intensities and binding energies of the hydrogen cluster ions.

However, detailed dynamical information is only available for the smallest cluster, H_5^+. Here, a H_3^+–H_2 structure with a very shallow potential energy surface and a great mobility of the central proton is predicted [10]. At full CI level of theory a harmonic vibrational frequency of 478 cm^{-1} ($\approx$ 59.3 meV) for the corresponding coordinate is predicted. The experimentally determined binding energy for this complex is 300 meV [7]. In the most extensive theoretical study up to date, Yamaguchi and coworkers calculated ten low lying stationary points at eleven levels of theory for H_5^+ [15]. For the migration of the central proton between the two H_2 a barrier of only 6.5 meV is predicted at (4s2p) CISD level, of 3.7 meV at (4s2p) full CI level and of 15 meV at (6s3p) CISD level of theory. Although detailed knowledge of intramolecular dynamics, especially for larger clusters, is missing to date a lot can be learned when adapting results for H_5^+ and extending these to larger assembles.

In a previous study we investigated growth and fragmentation of hydrogen cluster ions at a nominal temperature of 10 K with normal and para hydrogen tar-

[1] Corresponding author.

PII S0301-0104(96)00160-7

gets [17]. Rate coefficients for ternary association of smaller clusters (H_n^+, $n < 9$) in reaction with para hydrogen target turned out to be extremely large as compared to the association reaction with normal hydrogen, whereas for larger (H_n^+, $n \geqslant 9$) clusters the association rates are comparable for the two targets. To explain these results we extended the commonly accepted concept of the closure of the first cluster shell at a size of H_9^+ [7,11,16,18]. This concept is based on experimentally determined energetics and calculated equilibrium structures. We proposed a dynamical shell structure for hydrogen clusters: For smaller clusters an approaching ortho hydrogen molecule can transfer its rotational energy to the cluster. As this energy transfer requires an ortho–para transition in the target, an efficient proton exchange between the cluster and approaching hydrogen molecules must be possible. For larger clusters starting with H_9^+ this exchange is much less efficient due to closure of the first cluster shell.

In the present experiment we explore the dynamics of these interesting clusters some more and use D_2 as an isotopic tracer. When hydrogen clusters are stored in D_2-gas, at conditions where growth or fragmentation are negligible in first order, hydrogen is replaced by deuterium. This isotopic fractionation is caused by slightly different zero point energies of the deuterated versus the non-deuterated species. The rate of this process at different stages of deuteration progress for parent clusters of different size reveals information on the cluster structure and dynamics.

2. Experimental

The dynamics of the deuteration of hydrogen cluster cations was studied in a cooled 22-pole radio-frequency (RF) ion trap. This trap is part of a guided beam apparatus, that was described in detail in a previous publication [17]. Hydrogen cluster ions were created in a cooled corona discharge cluster ion source from high purity hydrogen (Messer-Griesheim, 5.0) that was further purified by means of a liquid nitrogen cooled molecular sieve. Ion source and trap were cooled by a Gifford–McMahon-type closed-cycle cryocooler (Leybold, RGD 210) providing 2 W of cooling power at 15 K. Clusters were mass selected by a first quadrupole and injected into the ion trap. The ions were stored for selected periods of time (ms to s) in deuterium target gas at a nominal temperature of 10 K. When necessary, He buffer gas was added to insure proper relaxation and cooling of the parent clusters. After extraction from the trap the ions were mass analyzed by a second quadrupole mass filter and detected by single ion counting via a Daly type detector. Each time typically 100 ions were injected into the trap and the number of products of 30 to 50 iterations were accumulated for each storage time and mass. When the ions are injected into the trap typically 10 to 100 collisions with buffer (or target) gas are needed for proper cooling and relaxation. The maximum number density of neutrals in the trap is limited to a value of approximately 10^{14} cm^{-3}. Assuming a Langevin rate coefficient for the thermalizing collisions ($\approx 10^{-9}$ cm^3 s^{-1}), several hundred microseconds up to a few milliseconds are needed for proper thermalization of the ions. As the process of deuteration turns out to be rather fast, proceeding nearly at the collision rate, the deuterium density had to be limited to a value of $\approx 3 \times 10^{11}$ cm^{-3} to allow observation of the first deuteration steps. Under these conditions it was necessary to add buffer gas (He or H_2) to insure proper injection and thermalization of the ions.

The target gas number density at high pressure is measured by a spinning rotor gauge (MKS quoted accuracy better than 5%). For experiments at very low target gas number densities (trap pressure $p < 10^{-5}$ mbar) an ionization gauge is used. The ion gauge is calibrated by the spinning rotor gauge in the overlapping pressure range. The uncertainty in the target gas number density is increased by a density gradient along the trap axis and especially by density fluctuations caused by slight variations of the trap temperature leading to condensation and re-evaporation of target gas. Therefore, we conservatively estimate the error in the absolute target gas density n to be $\pm$ 70% for the low density experiments and $\pm$ 50% for the high density experiments.

During the injection and subsequent thermalization process fragmentation of the weakly bound cluster ions cannot be avoided. For H_5^+ this effect is smaller than 10%, whereas for medium sized clusters (H_7^+, H_9^+) fragmentation becomes important and leads to a distribution of parent clusters. The effects of fragmentation have been carefully examined and cross checks with parent ions injected into helium buffer gas (equal mass as deuterium leading to a similar fragmentation

pattern) at comparable number densities have been performed.

At target gas number densities above 3×10^{12} cm^{-3} contributions from ternary association have to be considered. In these cases the growth of the largest injected parent cluster to the next larger cluster was monitored and even at the largest target and buffer gas number densities and longest storage times the influence of this effect on the measured ion intensities was less than 10%.

Stimulated by the results of our previous study here we investigated how the deuteration process is influenced when normal hydrogen or para hydrogen is used instead of helium as a buffer gas. These conditions lead to clusters with different internal excitation even at the same nominal temperature. However, such studies are simultaneously complicated by backreactions (D_2–H_2 exchange). Note that one obtains also minor contributions from backreaction in normal operation since the cluster ion source produces a continuous flow of normal hydrogen into the ion trap chamber. Under typical operational conditions a continuous admixture of $\approx 3\times10^{11}$ cm^{-3} of normal hydrogen in the 22-pole trap has to be accounted for.

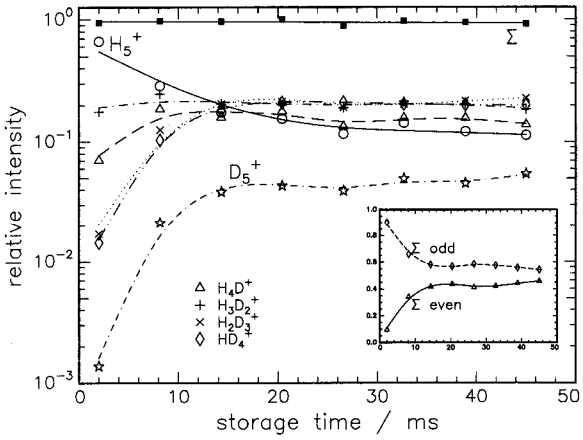

Fig. 1. Temporal evolution of the contents of the 22-pole ion trap following injection of H_5^+ into deuterium at a number density of 2.3×10^{11} cm^{-3} admixed to helium at a number density of 1.2×10^{14} cm^{-3}. In spite of the extremely low deuterium number density conversion of the parent ions proceeds extremely fast and equilibrium is reached after about 20 ms. Odd and even mass clusters are formed with comparable intensities. Even masses appear already at the first step of deuteration (H_4D^+, Δ). The insert shows the sum of odd and even mass contributions. A net transfer of odd to even masses is observed on the same time scale as the appearance of the fully deuterated species D_5^+. Full deuteration is not achieved due to backward reactions with H_2 (see text). All lines are spline fits to the experimental data and serve as a guide to the eye only.

3. Results

3.1. Raw data

Replacement of hydrogen by deuterium in cluster ions turns out to proceed extremely fast and very low deuterium number densities are sufficient (3×10^{11} cm^{-3}) to induce an efficient isotope exchange on the time scale of the trapping experiment. Fig. 1 shows the temporal evolution of H_5^+ parent clusters injected into deuterium target gas at a number density of 2.3×10^{11} cm^{-3} admixed to helium buffer gas at a number density of 1.2×10^{14} cm^{-3}. It takes only a few milliseconds for the H_5^+ to react to deuterated products. Note, that odd and even mass clusters are formed with comparable intensities. The early appearance of mass six (H_4D^+) exhibits, that already in the first step of deuteration the exchange of a single proton occurs with a rather large probability. Deuterated clusters appearing at odd masses ($H_3D_2^+$ and HD_4^+) can be created both by direct exchange of a D_2 molecule or by two subsequent exchanges of D atoms. Though these two reaction channels cannot be distinguished in our experiment, evidence will be provided below that they occur with comparable probability in the case of H_5^+. From the temporal evolution of the ion intensity it is apparent that the gain of the fully deuterated cluster (D_5^+) proceeds nearly as fast as reactive loss of the parent cluster (H_5^+). This means that for small clusters deuteration is an extremely fast process at all stages of deuteration progress. The corresponding rate constant for the decline of H_5^+ is close to the Langevin limit indicating that deuteration occurs with an efficiency close to unity. However, a closer inspection of the deuteration progress shows that the formation of clusters containing more than three D atoms (see Fig. 1 and 2) slows down due to back reaction (see below) after about 20 ms. The sum of odd numbered mass contributions (H_5^+, $D_2H_3^+$, and D_4H^+) as well as the even numbered counterpart (DH_4^+, $D_3H_2^+$, and D_5^+) is shown as an insert in Fig. 1. Interestingly these integral quantities show a similar temporal evolution

Table 1
Rate coefficients ($cm^3\ s^{-1}$) for the exchange of the first H_2, last H_2, last H and all outer H_2 in hydrogen clusters (details see text). k_L is the Langevin rate coefficient. Numbers in parentheses are powers of ten. Values given here are plotted in Fig. 6

	$k_{H_2}^{first}$	$k_{H_2}^{last}$	k_{H}^{last}	$k_{H_2}^{outer}$	k_L
H_3^+	$1.7 \pm 1.2(-9)$	-	-	-	$1.6(-9)$
H_5^+	$1.5 \pm 1.1(-9)$	-	-	-	$1.4(-9)$
H_7^+	$1.3 \pm 1.0(-9)$	-	-	-	$1.3(-9)$
H_9^+	$1.3 \pm 0.9(-9)$	$1.3 \pm 0.9(-10)$	$2.9 \pm 1.5(-12)$	$\gg 1.3(-10)$	$1.3(-9)$
H_{11}^+	-	$5.9 \pm 4.1(-11)$	$3.1 \pm 1.6(-13)$	$1.0 \pm 0.5(-9)$	$1.2(-9)$
H_{13}^+	-	$1.6 \pm 0.9(-13)$	$2.0 \pm 1.0(-13)$	$9.2 \pm 4.6(-10)$	$1.2(-9)$
H_{15}^+	-	$< 1.5(-14)$	$< 1.0(-13)$	$3.5 \pm 1.7(-10)$	$1.2(-9)$
H_{17}^+	-	$\ll 1.5(-14)$	$< 8.7(-14)$	$1.4 \pm 0.7(-1.0)$	$1.2(-9)$

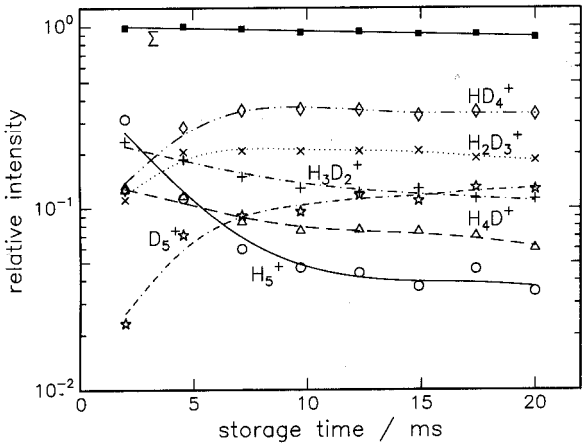

Fig. 2. Temporal evolution of the trap contents following injection of H_5^+. As in Fig. 1, the deuterium gas has a number density of 2.3×10^{11} cm^{-3}. Instead of He para hydrogen has been used as a buffer gas at a number density of 2.4×10^{13} cm^{-3}. Comparison with Fig. 1 reveals that the time constants are similar but that the stationary equilibrium concentrations are significantly influenced by the buffer gas.

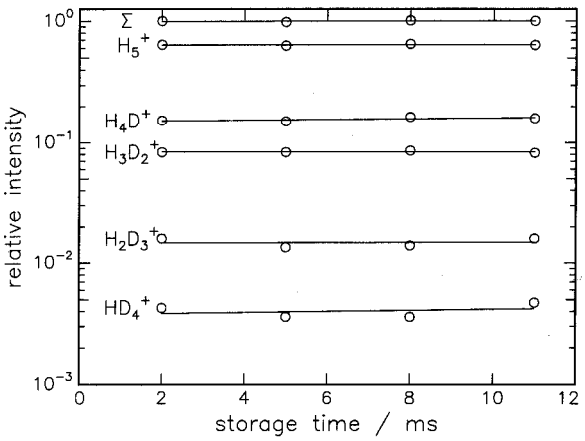

Fig. 3. Evolution of the trap contents following injection of H_5^+ into deuterium at a number density of 3.5×10^{11} cm^{-3} admixed to normal hydrogen at a number density of 2.6×10^{13} cm^{-3}. The deuterium number density is comparable to the number density of the measurement shown in Fig. 2. Almost all ions remain in the parent cluster channel indicating an efficient backward reaction in collisions with normal hydrogen as a buffer gas.

as the appearance of D_5^+ and the disappearance of H_5^+. A quantitative analysis of this behavior will be given in the next section (see Table 1) and discussed below. One of the main results of our previous study of cluster growth and fragmentation is the dramatically increasing rate constants for the growth of H_5^+ clusters when para hydrogen was used instead of normal hydrogen as a target gas. Therefore we also studied the influence of para hydrogen versus normal hydrogen as a buffer gas for the process of deuteration.

Deuteration in the presence of para hydrogen (p-H_2), see Fig. 2, is more efficient as compared to measurements with helium buffer gas (see Fig. 1). The initial conversion rate is similar (note the different scales in Figs. 1 and 2) but the higher degree of deuteration in Fig. 2 indicates a *colder* environment due to possible ortho-para transitions in H_5^+. In contrast a much different evolution is observed in the presence of normal hydrogen (n-H_2). Fig. 3 shows the temporal evolution of initially injected H_5^+ in n-H_2 at a number density of 2.6×10^{13} cm^{-3} admixed to D_2 at a number density of 3.5×10^{11} cm^{-3} (similar number density as in measurement shown in Fig. 2). In this case almost the total ion intensity remains at mass 5 (H_5^+) being evidence for a very efficient backward reaction induced

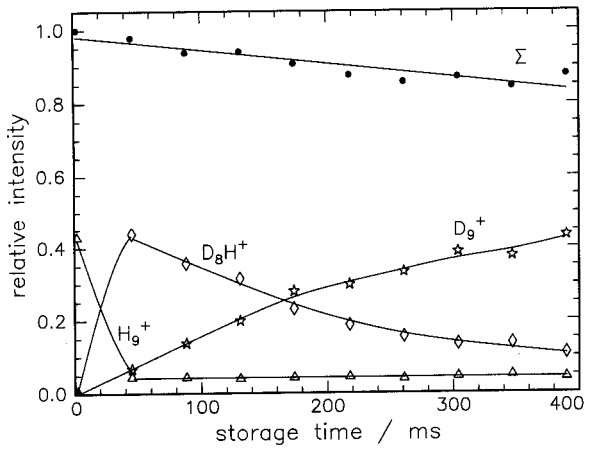

Fig. 4. Evolution of the trap contents following injection of H_9^+ into pure deuterium at a number density of 5×10^{12} cm^{-3} and a residual H_2 density of 3×10^{11} cm^{-3}. Deuteration of H_9^+ proceeds during the first 50 ms via the subsequent exchange of D_2 molecules until the D_8H^+ configuration is reached. The exchange of the last hydrogen happens on a much longer time scale. All other partially deuterated contributions have reached equilibrium and account for about 40% of the total ion intensity.

by the rotational energy of ortho hydrogen (o-H_2).

From a series of measurements at different n-H_2 number densities (much lower than in Fig. 3) we conclude that (see Section 3.2 below) the rate coefficient for the backward reaction is ten times smaller than the rate coefficient for deuteration. The efficient backward reaction in presence of normal hydrogen also explains the already mentioned slowing down of the deuteration process in Fig. 1 and Fig. 2. In these cases the deuterium number density and the normal hydrogen number density originating from the cluster ion source are comparable and further deuteration is counterbalanced by backward reactions. More efficient differential pumping of the cluster ion source will reduce this problem.

The next larger cluster which has been studied is H_7^+. In this case the temporal evolution is very similar to that of H_5^+ and therefore not shown. In contrast, when H_9^+ is injected into pure deuterium, the main features change dramatically as depicted in Fig. 4. The first steps of deuteration proceed very fast, too, but in these first steps the formation of even mass clusters (exchange of a single proton) is improbable. This means that deuteration proceeds via the exchange of molecular D_2 only (odd mass products exclusively) until the cluster has reached a mass of 17 amu (HD_8^+). In Fig. 4 only the major channels are shown for the sake of clarity; in the total ion sum all channels are accounted for. The slow increase of the even mass clusters corroborates the inefficiency of the proton–deuteron (p–d) exchanges. When the cluster has reached a mass of 17 amu the exchange process slows down dramatically. The exchange of the last proton in the cluster happens about 1000 times slower than the first deuteration steps. Therefore the time scale for the appearance of D_9^+ is on the order of hundreds of milliseconds as compared to milliseconds for the loss of H_9^+. Note that the target gas density in this experiment was more than ten times larger than for the deuteration of H_5^+. These large differences allow us to separate the different steps of deuteration and thus to derive rate coefficients for these steps which will be discussed below (see Table 1).

For clusters larger than H_9^+ measurements are more complicated due to the fact that the outer H_2's are bound more weakly to the cluster. Therefore significant fragmentation occurs upon injection resulting in a wide mass distribution of parent clusters. As a consequence the mass spectra of deuterated products are congested, i.e. deuterated products of fragments and parent clusters contribute to the same mass peak (e.g. $H_{11}D_2^+$ and H_{15}^+). In addition more care has to be taken not to induce ternary association (i.e. cluster growth) during the trapping period since the ternary rate coefficients are larger than for the smaller clusters [17].

Despite all these problems additional interesting features have been derived from the deuteration of higher mass parent clusters. This is demonstrated for the injection of H_{15}^+ into pure D_2 in Fig. 5. After a few hundred microseconds we find a cluster mass distribution of approximately 25% H_9^+, 25% H_{11}^+, 25% H_{13}^+, 20% H_{15}^+. The initial congestion is becoming untangled after a trapping time of several milliseconds, because the first steps of deuteration proceed extremely fast. The largest parent cluster H_{15}^+ re-appears on mass 27 amu ($H_3D_{12}^+$) indicating that all H_2 of the cluster with exception of the H_3^+ core have been replaced by D_2. This process is almost completed after a trapping period of 200 ms. The smaller clusters (9,11, and 13) evolve into a distribution ranging from mass 17 to mass 26 and the separation of two neighboring clusters, $\Delta m = 2$, is transformed into a separation of the fully deuterated clusters of $\Delta m = 4$. This difference is

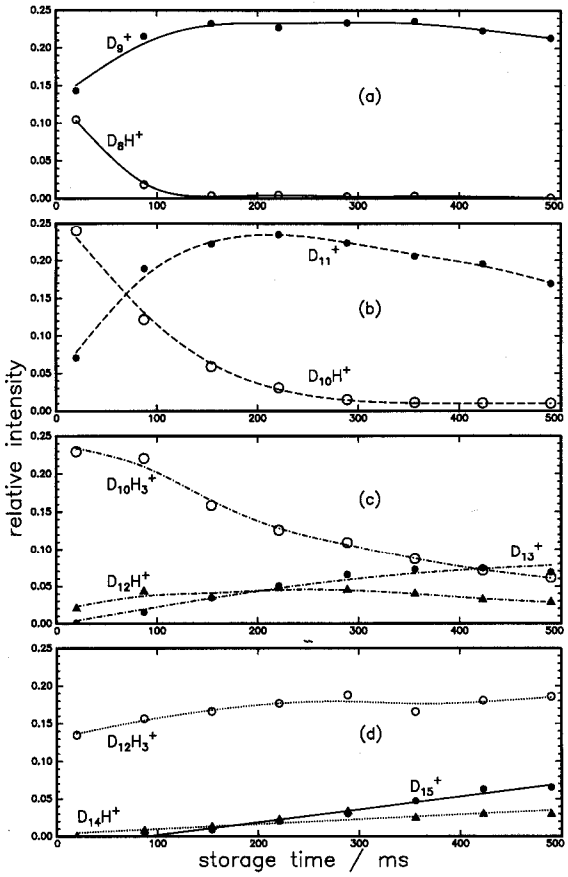

Fig. 5. Evolution of the trap contents following injection of H_{15}^+ into pure deuterium at a number density of 2.7×10^{12} cm^{-3}. Fragmentation following the injection process leads to an initial distribution of parent ions. From experiments in pure helium at the same number density and from the intensity of the fully deuterated clusters we find that the initial trap contents consists of 25% H_9^+ (a), 25% H_{11}^+ (b), 25% H_{13}^+ (c) and 20% H_{15}^+ (d). Due to a mass separation of $\Delta m = 4$ of the partially deuterated clusters the temporal evolution of the individual parent clusters can be traced. Details are explained in the text. Note that for H_{15}^+ complete deuteration becomes nearly impossible at the time scale and density of this experiment.

large enough to distinguish and assign all contributing cluster sizes as shown in Figs. 5a–5d. At storage times of several hundred milliseconds initially stored H_9^+ clusters appear on mass 17 (HD_8^+) and 18 (D_9^+) only. As has been found for the smaller clusters (H_5^+ and H_7^+) not only peripheral H_2 subunits have been exchanged in H_9^+ but also two nuclei of the proposed H_3^+ cluster core [7]. Under the experimental conditions of Fig. 5 only the last step of deuteration (i.e. exchange of the last proton) is observed. The next larger cluster H_{11}^+ appears mainly on mass 21 (HD_{10}^+) finally ending up on mass 22 (D_{11}^+). Therefore it exhibits the same final reaction step as could be seen for H_9^+. Initially stored H_{13}^+ clusters appear mainly on mass 23 ($H_3D_{10}^+$). This contribution evolves slowly via mass 25 (HD_{12}^+) to reach finally mass 26 (D_{13}^+). This finding shows that the insertion of D_2 molecules into the cluster core becomes slower for larger clusters. For H_{15}^+ this process appears to be almost impossible, as most of the initially stored H_{15}^+ clusters remain at mass 27 ($H_3D_{12}^+$). This may indicate that entering the H_3^+ core of the cluster becomes less likely the larger the cluster. But the observation may also be due to the fact that the D_2–H_2 backreaction is more efficient for peripheral molecules (more details are given in Section 4).

3.2. Kinetics of the deuteration process

The kinetics of the process of deuteration of a specific cluster size can be described by a set of coupled differential equations. In our previous study [17] we have demonstrated how a simulation of our experimental data yield reliable rate coefficients for growth and fragmentation of hydrogen cluster ions in H_2. In the present study it is not straight forward to apply this method for the following reasons. For small clusters the sequential exchange of one proton only could be distinguished from the exchange of a complete H_2 at extremely low target gas densities. Corresponding measurements are planned. For larger clusters the congestion problem mentioned before would have to be solved by mass selection of the fragments after thermalization (resonant excitation). This method was not applied in the present study. However, the fact that the process of deuteration happens on extremely different time scales enables us to gather rate coefficients for a few basic reaction steps.

For small clusters (i.e. H_5^+ and H_7^+) the isotopic exchange reaction is very fast. Exponential fits for the loss of the parent mass ($k_{H_2}^{first}$) and the gain of the fully deuterated clusters ($k_{H_2}^{last}$ and k_H^{last}) can be employed to derive rate coefficients for these important steps. Results from this analysis are summarized in Table 1 and plotted in Fig. 6. All rate coefficients for the first deuteration steps are close or equal to the Langevin

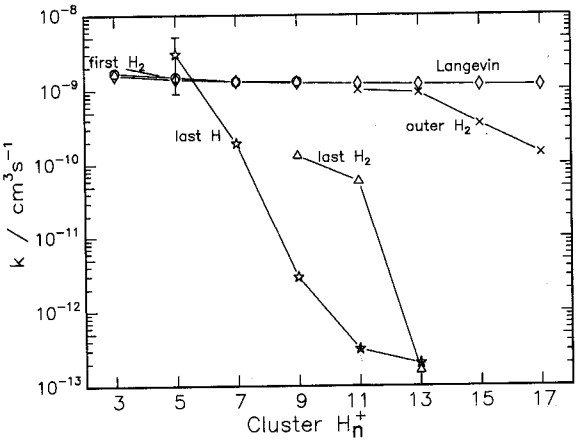

Fig. 6. Rate coefficients at different stages of deuteration as a function of the parent cluster size. The exchange of the first H_2 or outer H_2 is calculated from the rate of disappearance of the parent cluster. A comparison to the Langevin rate coefficient reveals that initial deuteration proceeds almost at the collision rate. The rate of exchange of the last H_2 is determined from the rate of appearance in the $H_{n-1}D^+$ channel and the rate of exchange of the final proton (last H) from the rate of formation of D_n^+. For details on the analysis of these rate coefficients see text.

collision rate coefficients (k_L, also listed in Table 1) implying that every collision leads to deuteration either by exchange of one proton or a H_2 molecule.

For the first closed shell cluster, H_9^+, and larger clusters (e.g. H_{15}^+) the essential information can be obtained in a similar way. Again, the first steps of deuteration happen extremely fast (not visible on the time scale of the measurement shown in Fig. 5). Therefore, the rate of loss of parent molecules ($k_{H_2}^{outer}$) is the key figure for the initial step. In addition, the exchange of a H_2 molecule is significantly favoured as compared to the exchange of a single proton. The subsequent process of deuteration remains fast until the exchange of the last proton. Here the process slows down dramatically. Due to overlapping masses from neighbour parent clusters it is difficult to derive reliable values for these intermediate steps. However, the gain in the bottleneck channel gives an upper limit for all steps of deuteration in between. The corresponding rate coefficient, $k_{H_2}^{last}$, is a measure for the efficiency of the exchange of the last H_2 in the parent cluster. Respective rate coefficients are also summarized in Table 1. After almost all intensity has reached the bottleneck channel the fully isotopically exchanged cluster is formed on a much longer time scale. The corresponding rate coefficient, k_H^{last}, is a measure for the exchange of the last proton in the parent cluster.

4. Discussion

Our previous study on the dynamics of growth and fragmentation of hydrogen cluster ions in pure hydrogen [17] revealed a large size effect for rate coefficient of cluster growth when using p-H_2 as a target. In addition ortho–para transitions in the H_2-target molecules, mediated by scrambling collisions, play a significant role. It is the aim of the present work to obtain some more detailed information on the intracluster motions involved when hydrogen is replaced by deuterium in this class of cluster.

At the low temperature of our experiments the internal energy of a fully thermalized parent cluster (H_n^+, $n < 19$) is fairly low as compared to the binding energy of the last H_2. Therefore the parent cluster can be considered to be close to its equilibrium structure. When a D_2 approaches this cluster its binding energy and the collision energy are available as internal energy of the collision complex. If the complex is not stabilized by third body collisions or radiation (can be ignored in the current experiment) it has to decompose because the internal energy is above the dissociation limit. In a simple shell model the internal energy can be distributed among equivalent molecular subunits (H_3^+ core, H_2 molecules and one D_2 molecule in the first step of deuteration). Therefore decomposition into $H_n^+ + D_2$ or $H_{n-2}D_2^+ + H_2$ has to be considered.

Our experiment clearly shows that the latter product channel is strongly favourized. Almost every collision leads to a long lived complex and an exchange of hydrogen by deuterium. In the first step of deuteration there are more equivalent H_2 than D_2 favouring the ejection of one of those. However, even after several H_2 have been replaced and the statistical weight is in favour of the D_2 products, deuteration does not slow down significantly as can be seen from our experiments (see Fig. 6).

In this simple statistical consideration H_2 and D_2 were considered equivalent molecular subunits of the collision complex. More important, however, is the difference in zero point energy of the molecule–cluster motion. It is the energy gain of this exchange reac-

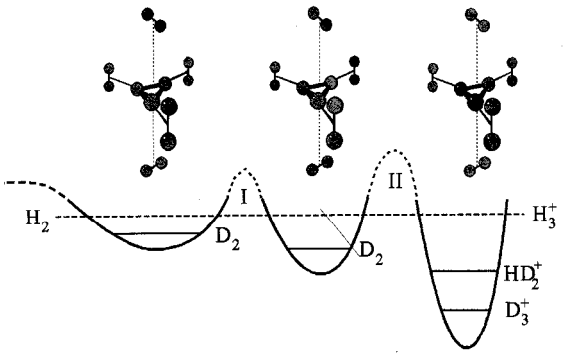

Fig. 7. Schematic view of proposed dynamical shell structure for the example of a H_{13}^+ cluster. The potential energy diagram is drawn for the initial step of deuteration. The dashed line indicates that no energy is gained when exchanging inner H_2 by outer H_2. Possible ground states for D_2 at various positions within the cluster (shown in the cluster structure above) are given as solid lines in the diagram. The dynamics of deuteration are explained in the text.

tion which favourizes a deuteration. A crude potential energy diagram for the initial step of deuteration for a hydrogen cluster ion (as an example H_{13}^+) is shown schematically in Fig. 7. According to the shell structure all H_2 molecules in outer shells and the H_3^+ core are energetically degenerate because no energy can be gained from any hydrogen–hydrogen exchange within the cluster (dashed line). The constituents of the cluster occupy inner and outer shells which are separated by energy barriers of increasing height (depicted as I and II in Fig. 7 schematically, no ab initio calculations exist) when penetrating deeper into the cluster. In addition inner hydrogens are bound more tightly than peripheral molecules. Experimental values for the binding energy of the outermost H_2 have been determined by Hiraoka ranging from 300 meV for H_5^+ down to 67 meV for H_{15}^+ [7]. In another experiment Hiraoka and Mori measured the difference in binding energy for hydrogen clusters as compared to deuterium clusters [9]. They derive values of 21 meV for X_5^+, 13 meV for X_7^+ and 6.5 meV for X_9^+ and larger clusters. As a consequence the energy gain for deuteration (in the outer shell) is decreasing for larger clusters. Therefore the general trend of a slowing down of the exchange of the outer H_2 is expected when the energy gain of deuteration is becoming smaller than the collision energy. A comparison with our experimental results (see $k_{H_2}^{outer}$ in Fig. 6) reveals that this situation is reached for clusters larger than H_{13}^+.

After the first step of deuteration we find no evidence for a slowing down of the deuteration process except for the exchange of the final H_2 and/or final proton. Therefore the energy gain of the steps following the first exchange must be comparable to the initial deuteration. On the one hand this would be expected for the sequential replacement of equivalent molecular units from the outer shell. On the other hand the statistical weight discussed earlier should reduce the efficiency of deuterating products, especially for larger clusters with more equivalent molecules. This rate reducing effect can be disregarded provided that peripheral D_2 in the first cluster shell is able to exchange with inner H_2 (internal deuteration) before it collides with the next D_2. In this case an approaching D_2 finds always an outer shell with H_2. Energetically this process is favourable since the energy gain of deuteration is larger for inner molecules. In Fig. 7 this is shown schematically since no accurate experimental or theoretical data are available to date. However, ignoring the bond energies of the core H_3^+ to surrounding H_2 molecules one can estimate the energy gain from the deuteration process in the core of a cluster to be given by the well studied reaction:

$$\begin{aligned} H_3^+ + D_2 &\rightarrow HD_2^+ + H_2, \qquad \Delta H^0 = -21 \text{ meV}, \\ &\rightarrow H_2D^+ + HD, \qquad \Delta H^0 = -4.9 \text{ meV}. \end{aligned} \tag{1}$$

The ΔH^0 values given here are due the zero point energy differences [19]. This value is much larger than the energy gain of deuteration of the outermost H_2 in H_9^+ of 6.5 meV. A comparison of the H_2 and D_2 bond energies in pure hydrogen or deuterium clusters is given by Hiraoka and Mori [9]. We take this as a motivation for the general trend shown in Fig. 7.

Unless backreaction with residual H_2 plays a significant role, which will be discussed below, deuteration proceeds until all hydrogen molecules are replaced by deuterium (for H_n^+, $n < 15$). This shows that deuteration of inner shells, a unimolecular rearrangement process, takes place although it might be hindered by barriers as denoted in Fig. 7. As long as the time needed to overcome the barrier via tunneling is short compared to the collision time (in this experiment on the order of milliseconds) a H_2 molecule can be replaced by D_2 in each collision.

Under the present experimental conditions we find

a reduced reaction rate only for the exchange of the final H_2 ($k_{H_2}^{last}$) and final proton (k_H^{last}) which both belong to the H_3^+ cluster core, the innermost shell of the proposed structure. Hence we take this as evidence that barrier I (see Fig. 7) can be overcome at the conditions of the present experiment (energy, collision rates with D_2) in contrast to barrier II. Therefore we believe that deuteration of larger clusters (H_n^+, $n \geqslant 9$) starts with the outermost shell, then D_2 penetrates the cluster until all shells except for the H_3^+ core are perdeuterated.

Great differences are found for the deuteration of smaller clusters (H_5^+ and H_7^+) as compared to larger assembles. Here we do observe the exchange of atomic and molecular hydrogen already in the first step. The reaction mechanisms for the deuteration of the H_3^+ core seem to be similar. Differences arise from the fact that for smaller clusters the core is accessible more easily. Here, the insertion of one D_2 into the cluster core proceeds very fast. This can be explained by an efficient proton transfer between the core and the H_2/D_2 at the corners of the inner H_3^+ triangle. As has been shown for H_5^+ [10] the proton can then be forming a new HD_2^+ core with peripheral H_2/D_2. However, only D_2 molecules as a whole can be incorporated via this proton jump mechanism.

Although the natural abundance of HD is fairly low residual HD could be built in the same way leading to H_2D^+ and finally (with another D_2 insertion) to the fully deuterated D_3^+ core. This way only the molecular exchange process is necessary to explain the deuteration of the hydrogen cluster ions. Due to the very fast reaction in small clusters and the fairly low HD abundance this seems to be unlikely for those species. Interestingly for clusters larger than H_7^+ the perdeuterated cluster (D_n^+) is the only even numbered species observed. This excludes the presence of an HD-intermediate ($H_2D_{n-2}^+$, backreaction of HD_{n-1}^+ with HD) which would be expected to arise during the long time passed prior the final step of deuteration of the HD_{n-1}^+ precursor. Therefore we believe that HD is playing only a minor role in the deuteration process.

Another internal motion has to be active to allow for the efficient single proton exchange, i.e. proton scrambling. For H_5^+ Ahlrichs pointed out, that this might be an in-plane rotation of the H_3^+ subunit [10]. This intramolecular motion is hindered by a barrier of 150 meV. As this is well below the dissociation limit of this particular cluster, this mechanism is a possible way for an effective proton transfer. For larger clusters this internal motion seems very unlikely. While the available energy is decreased significantly, the barrier for the in-plane rotation of the central H_3^+ can be expected to be increased, because the number of bonds increases. Therefore we propose a second core rearrangement. In a partially deuterated cluster this might occur via a proton or a deuteron. Whereas the former leads to a H_3^+ core the latter gives a H_2D^+ core surrounded by a H_2/D_2 and a HD. In case the HD unit leaves the cluster the proton transfer is finally completed. All other exit channels lead to an H_2–D_2 exchange.

The efficient proton rearrangement of the central proton or H_3^+ core does also play an important role in the interaction of the cluster with o-H_2 and p-H_2. In our previous study we found a substantial heating in scrambling collisions with o-H_2 containing n-H_2. This effect leads to a large increase of the backward reaction observed for the deuteration of H_5^+ in D_2 with an addition of n-H_2 (see Fig. 3). In contrast our measurements with an addition of the p-H_2 (see Fig. 2) show a cooling effect. A comparison to measurements with additional helium (see Fig. 1) reveals that deuteration becomes even more complete in p-H_2. This leads us to the conclusion that scrambling collisions cannot only heat the cluster (ortho–para transitions in the cluster: $\Delta E = +14$ meV) but also the reverse process seems possible.

5. Summary and outlook

In the present study deuterium was used as an isotopic tracer to reveal information on structure and intramolecular dynamics of hydrogen cluster cations. The rate coefficients for the exchange of a single proton turned out to be surprisingly large for small clusters and to decrease dramatically with increasing cluster size. Also the exchange of complete hydrogen molecules shows significant size effects. These results serve as strong evidence for our previously proposed dynamical shell model [17] which is consistent with previous experiments [7,18]. For a deeper understanding of the dynamical effects in these clusters potential energy surfaces or at least low lying stationary points for clusters larger than H_5^+ are urgently needed.

It turned out that in spite of the shallow potential energy surfaces of these clusters, the concept of equilibrium structure remains useful and can help to interpret even dynamical processes. Based on the equilibrium structures and extrapolating from the dynamical properties of the well studied H_5^+ we propose three mechanisms to explain the process of deuteration in hydrogen cluster cations: a direct exchange of a complete molecule in the outer shell followed by an internal deuteration in which molecules from an outer shell can invade the inner part of the cluster. The insertion of a molecule into the cluster core is proceeding via a proton transfer including internal rearrangement.

The exchange of single protons is responsible for the efficient heating of small clusters in collisions with o-H_2. This effect has been observed already in our previous study [17]. The reverse effect, cooling, has been observed when p-H_2 is used as a buffer gas, and results in a more complete deuteration.

The investigations could be extended into different directions to derive more dynamical information. From the investigation of larger clusters one could learn more about the closure of a second shell which is expected to arise at a cluster size of H_{15}^+ [9]. Due to decreasing binding energies we expect the intracluster exchange of hydrogen subunits to become more efficient. Therefore the use of para versus normal deuterium could reveal similar shell effects as in the case of hydrogen and might help to explain the unexpectedly low value for the difference in the binding energy of deuterium and hydrogen cluster ions [9]. Interesting experiments could be performed at very low densities or with pulsed target gas. Such experimental conditions would allow to follow the evolution of the internal rearrangement. According to the tentative energetics given in Fig. 7 even the metastable decay following the insertion of a peripheral D_2 into the core should be observable. Detailed information on reaction probabilities can be obtained from low energy collisions in a merged beam apparatus. First experiments for the $H_3^+ + D_2 \rightarrow DH_2^+ + HD$, $D_2H^+ + H_2$ have been carried out recently [20,21].

Acknowledgements

This work was supported by the Deutsche Forschungsgemeinschaft (Innovationskolleg INK 2, Chemnitz) and the European Community (Human Capital and Mobility program) under contract number ERBCHRXCT930150.

References

[1] R. Clampitt and L. Gowland, Nature 223 (1969) 815.
[2] U.A. Arivof, S.L. Pozhavov, I.G. Chernov and Z.A. Mukhamediev, High Energy Chem. (USSR) 5 (1971) 69.
[3] S.L. Bennett and F.H. Field, J. Am. Chem. Soc. 94 (1972) 8669.
[4] A. van Deursen and J. Reuss, Intern. J. Mass Spectrom. Ion Phys. 27 (1973) 197.
[5] K. Hiraoka and P. Kebarle, J. Chem. Phys. 62 (1975) 2267.
[6] A. van Lumig and J. Reuss, Intern. J. Mass Spectrom. Ion Phys. 27 (1978) 197.
[7] K. Hiraoka, J. Chem. Phys. 87 (1987) 4048.
[8] N.J. Kirchner and M.T. Bowers, J. Phys. Chem. 92 (1987) 2573.
[9] K. Hiraoka and T. Mori, Chem. Phys. Letters 157 (1989) 467.
[10] R. Ahlrichs, Theoret. Chim. Acta 39 (1975) 149.
[11] Y. Yamaguchi, J.F. Gaw and H.F. Schaefer III, J. Chem. Phys. 78 (1983) 4074.
[12] B. Farizon, M. Farizon, H. Chermette and M.J. Gaillard, submitted to J. Chem. Phys. (1995).
[13] S. Yamabe, K. Hirao and K. Kitaura, Chem. Phys. Letters 56 (1978) 546.
[14] K. Hirao and S. Yamabe, Chem. Phys. 80 (1980) 237.
[15] Y. Yamaguchi, J.F. Gaw, R.B. Remington and H.F. Schaefer III, J. Chem. Phys. 86 (1987) 5072.
[16] M. Farizon, H. Chermette and B. Farizon-Mazuy, J. Chem. Phys. 96 (1992) 1325.
[17] W. Paul, B. Lücke, S. Schlemmer and D. Gerlich, Intern. J. Mass Spectrom. Ion Processes 150 (1995) 373.
[18] M. Okumura, L.I. Yeh and Y.T. Lee, J. Chem. Phys. 88 (1988) 79.
[19] N.G. Adams and D. Smith, in: Reactions of small transient species: kinetics and energetics, eds. A. Fontijn and M.A.A. Clyne (Academic Press, New York, 1983) p. 311.
[20] D. Gerlich, H.J. Jitschin and O. Wick, in: Symposium on Atomic and Surface Physics, eds. D. Bassi et al., Pampeago/Italy, 1992.
[21] O. Wick, Untersuchungen von Ionen-Molekülreaktionen bei extrem niedrigen Energien mit zustandsselektiv präparierten Reaktanden, PhD Thesis, Universität Freiburg (1994).